NUMERICAL ANALYSIS OF OPEN CHANNEL STEADY GRADUALLY VARIED FLOW USING THE SIMPLIFIED SAINT-VENANT EQUATIONS

WOJCIECH ARTICHOWICZ

Department of Hydraulic Engineering,
Faculty of Civil and Environmental Engineering,
Gdansk University of Technology,
Narutowicza 11/12, 80-233 Gdansk, Poland
wojartic@pg.gda.pl

Abstract: For one-dimensional open-channel flow modeling, the energy equation is usually used. There exist numerous approaches using the energy equation for open-channel flow computations, which resulted in the development of several very efficient methods for solving this problem applied to channel networks. However, the dynamic equation can be used for this purpose as well. This paper introduces a method for solving a system of non-linear equations by the discretization of the one-dimensional dynamic equation for open-channel networks. The results of the computations using the dynamic and energy equations were compared for an arbitrarily chosen problem. Also, the reasons for the differences between the solution of the dynamic and energy equation were investigated.

Keywords: dynamic equation, open-channel flow, open-channel networks, steady flow

1. Introduction

In engineering practice, we very often face the problem of steady, gradually varied (SGV) flow in open channels. The governing equation for this kind of flow can be derived from the Bernoulli equation [1]. To this effect, let us consider the situation presented in Figure 1.

When considering two neighboring cross-sections one can write the following equation of mechanical energy conservation:

$$z + H + \frac{\alpha \cdot U^2}{2g} = (z - s \cdot dx) + (H + dH) + \frac{\alpha(U + dU)^2}{2g} + S \cdot dx \tag{1}$$

where:

x – space coordinate,

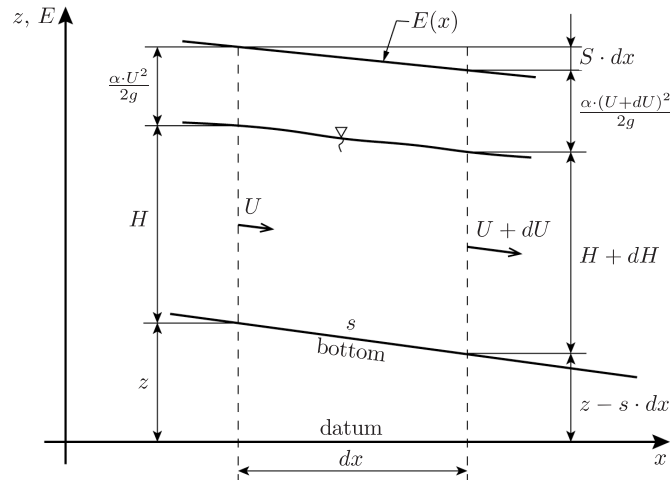z – bed elevation with regard to the datum,

Figure 1. Derivation of energy equation

H – depth,

U – average flow velocity,

s – bottom slope,

S – friction slope,

g – gravitational acceleration,

α – energy correction factor.

     The squared velocity at the downstream end can be expressed using the approximate formula:

$$(U+dU)^2 = U^2 + 2U \cdot dU + (dU)^2 \approx U^2 + 2U \cdot dU \tag{2}$$

By introducing this relation into Equation (1) one obtains:

$$s = \frac{dH}{dx} + \frac{\alpha}{g}\frac{U \cdot dU}{dx} + S \tag{3}$$

After simple rearrangements it takes the following form:

$$\frac{d}{dx}\left(h + \frac{\alpha \cdot Q^2}{2g \cdot A^2}\right) = -S \tag{4}$$

with:

$$h = H + z \tag{5}$$

and

$$Q = U \cdot A \tag{6}$$

where h denotes the water stage, A is the wetted cross-section area and Q is the flow discharge. The friction slope S usually is estimated using the Manning's formula:

$$S = \frac{Q^2 \cdot n^2}{R^{4/3} \cdot A^2} \tag{7}$$

in which n is Manning's roughness coefficient and R is the hydraulic radius.

Ordinary differential Equation (4) describes the flow profile along the channel axis, which is a solution obtained from a problem properly formulated for this equation.

Open-channel flow can be considered to be either steady or unsteady. Steady flow, however, can be regarded as a particular case of unsteady flow. For this reason, Equation (4) describing SGV flow can also be obtained in other ways. Namely, it can be derived from the Saint-Venant equations, which describe unsteady flow in open channels. A system of Saint-Venant equations consists of the mass conservation (continuity) equation and the momentum conservation (dynamic) equation. When lateral inflow is neglected, these equations take the following form:

$$\frac{\partial A}{\partial t} + \frac{\partial Q}{\partial x} = 0 \tag{8}$$

$$\frac{\partial Q}{\partial t} + \frac{\partial}{\partial x}\left(\frac{\beta \cdot Q^2}{A}\right) + g \cdot A \cdot \frac{\partial h}{\partial x} = -g \cdot A \cdot S \tag{9}$$

where t is time, β is momentum correction factor (assumed to be constant). A detailed derivation of the Saint-Venant equations is given by many authors (*e.g.* in [2] and [3]).

If the flow parameters do not change with time, as is the case with steady flow, the derivatives with respect to time vanish. In such a case, Equations (8)–(9) are reduced to the following form:

$$\frac{dQ}{dx} = 0 \tag{10}$$

$$\frac{d}{dx}\left(\frac{\beta \cdot Q^2}{A}\right) + g \cdot A \cdot \frac{dh}{dx} = -g \cdot A \cdot S \tag{11}$$

Since these equations give a general description of SGV flow, it seems that they can be used directly for modeling this kind of flow. Comparing their solutions with the solution of Equation (4) can be particularly interesting. This paper attempts to apply Equations (10)–(11) to the modeling of SGV flow in an open-channel network.

2. Problem statement

The problem of solving Equations (10)–(11) can be considered differently depending on the available information about the flow discharge Q. If Q is known, then the solution of Equation (10) is obvious: the flow discharge along the channel axis is constant, $Q = \text{const}$. In such a case the flow profile is obtained by solving Equation (11) with given initial condition:

$$h(x=0) = h_0 \tag{12}$$

In other words, the flow profile is a solution of initial value problem for the ordinary differential equation (11).
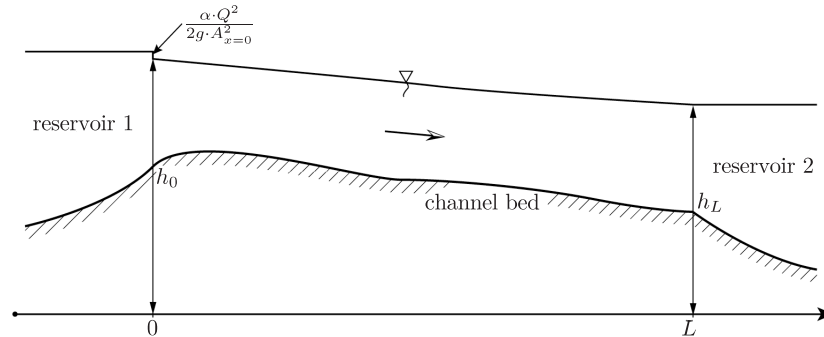
Figure 2. Channel connecting two reservoirs

A different approach must be applied in the case when Q is unknown. In such a case for the system of Equations (10)–(11), a two point boundary value problem (BVP) must be formulated.

The flow profile $h(x)$ must satisfy the governing equations (10)–(11) as well as the two conditions imposed at both ends of the considered channel. A typical example of a BVP formulated for a single channel is shown in Figure 2. The considered channel connects two reservoirs with different, but time-independent, water levels. The flow profile in the channel and the flow rate Q can be obtained by solving Equations (10)–(11) with the following boundary conditions:

$$h(x=0) = h_0 + \left.\frac{\alpha \cdot Q^2}{2g \cdot A^2}\right|_{x=0} \tag{13}$$

$$h(x=L) = h_L \tag{14}$$

A detailed description of the problem presented above can be found in [1]. As long as a single channel is considered, the boundary conditions (13)–(14) allow us to solve Equations (10)–(11). To this effect, any method suitable for BVP can be used [1]. Therefore, the shooting or difference method can be applied [4]. The situation is different for SGV flow in a channel network.

Figure 3. Open-channel network
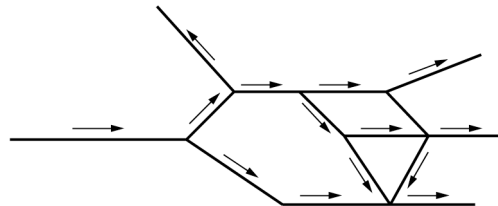
Let us consider a network shown in Figure 3. In this case, the shooting method is rather ineffective and it can be applied only in certain cases. Alternatively, we can use the complete Saint-Venant equations with imposed time-independent boundary conditions or apply the difference method to Equation (4) or (11). Solving the complete Saint-Venant equations seems to be very inefficient

for this purpose. Typically, the difference method is the most effective. However, in order to obtain the solution of the SGV flow equations for an open-channel network, certain conditions must be prescribed at the channel junctions, apart from the boundary conditions imposed at the ends of the pendant channels. Namely, for a junction such as that presented in Figure 4 we can formulate two additional relations resulting from the energy and mass conservation principles.
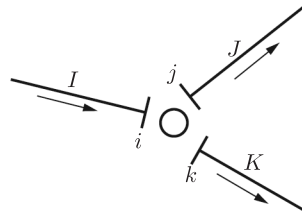

Figure 4. Junction connecting three channels

Assuming that the energy lines for the channels connected at the junction are at the same level, the following equations can be written:

$$h_{I,i} + \frac{\alpha_{I,i} \cdot Q_{I,i}^2}{2g \cdot A_{I,i}^2} = h_{J,j} + \frac{\alpha_{J,j} \cdot Q_{J,j}^2}{2g \cdot A_{J,j}^2} = h_{K,k} + \frac{\alpha_{K,k} \cdot Q_{K,k}^2}{2g \cdot A_{K,k}^2} \tag{15}$$

The subsequent relation results from the mass conservation principle. Assuming that the positive flow directions coincide with the arrows in Figure 4, the relation can be expressed as follows:

$$Q_{I,i} = Q_{J,j} + Q_{K,k} \tag{16}$$

In Equations (15)–(16) the subscripts I, J, K denote channel indicies whereas the subscripts i, j, k are the cross-section indicies.

The above relations, together with the boundary conditions (13)–(14), allow us to solve the SGV flow equations for any channel network, regardless of its type.

3. Numerical solution of SGV flow equations

To solve the BVP for the system of ordinary differential equations (10)–(11) the finite difference method (FDM) can be used. To this order the Ith channel which constitutes part of the network presented in Figure 3 and has the length L_I, is divided into $(N_I - 1)$ segments with constant lengths Δx, where N_I denotes the number of cross-sections. An approximation for a single interval limited by nodes i and $i+1$ is assumed, as shown in Figure 5.
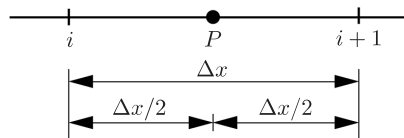

Figure 5. FDM discretization scheme, where P is the point of approximation

All derivatives presented in Equation (11) are approximated using central differences at point P, which is located in the middle of the segment. Consequently, we obtain:

$$\frac{1}{g \cdot A_P} \frac{\beta \cdot Q^2}{\Delta x} \left(\frac{1}{A_{i+1}} - \frac{1}{A_i} \right) + \left(\frac{h_{i+1} - h_i}{\Delta x} \right) + S_P = 0 \tag{17}$$

where the subscript P denotes the values taken at point P. Therefore the respective values are given by:

$$A_P = \frac{1}{2}(A_i + A_{i+1}) \tag{18}$$

$$S_P = \left(\frac{|Q|Q \cdot n^2}{A^2 \cdot R^{4/3}} \right)_P = \frac{1}{2} \left[\left(\frac{|Q|Q \cdot n^2}{A^2 \cdot R^{4/3}} \right)_i + \left(\frac{|Q|Q \cdot n^2}{A^2 \cdot R^{4/3}} \right)_{i+1} \right] \tag{19}$$

The modulus of flow rate Q was introduced into Equation (19) in order to preserve the information about the flow direction.

Equation (17) together with Equations (18)–(19) can be rearranged to obtain:

$$h_{i+1} - h_i + \frac{2\beta \cdot Q^2}{g(A_i + A_{i+1})} \left(\frac{1}{A_{i+1}} - \frac{1}{A_i} \right) + \frac{\Delta x}{2} \left(\frac{|Q|Q \cdot n_i^2}{A_i^2 \cdot R_i^{4/3}} + \frac{|Q|Q \cdot n_{i+1}^2}{A_{i+1}^2 \cdot R_{i+1}^{4/3}} \right) = 0 \tag{20}$$

Since the Ith channel was divided into $(N_I - 1)$ segments, for each channel, we can write $(N_I - 1)$ similar equations. Consequently, we obtain a system of $(N_I - 1)$ equations containing $(N_I + 1)$ unknowns. The prescribed boundary conditions (13)–(14) must be introduced in order to close this system. Using matrix notation, the obtained system of equations is expressed as follows:

$$\boldsymbol{a}\boldsymbol{x} = \boldsymbol{b} \tag{21}$$

where $\boldsymbol{a}$ is the matrix of coefficients, $\boldsymbol{b}$ is the right-hand side vector, and $\boldsymbol{x}$ is the unknown vector, defined as follows:

$$\boldsymbol{a} = \begin{bmatrix} a_{1,1} & & & & & & \\ a_{2,1} & a_{2,2} & & & & & a_{2,N_I+1} \\ & & \ddots & \ddots & & & \vdots \\ & & a_{N_I-1,N_I} & a_{N_I-1,N_I-1} & & a_{N_I-1,N_I+1} \\ & & & & a_{N_I,N_I} & \\ & & & a_{N_I+1,N_I-1} & a_{N_I+1,N_I} & a_{N_I+1,N_I+1} \end{bmatrix} \tag{22}$$

$$\boldsymbol{x} = \begin{bmatrix} h_1 \\ h_2 \\ \vdots \\ h_N \\ Q \end{bmatrix}, \qquad \boldsymbol{b} = \begin{bmatrix} h_0 \\ 0 \\ \vdots \\ 0 \\ h_L \\ 0 \end{bmatrix} \tag{23}$$

The vector $\boldsymbol{x}$ contains (N_I+1) unknowns, *i.e.* N_I nodal values of water stages and the flow discharge Q in the Ith channel. The elements of the matrix $\boldsymbol{a}$ are the coefficients resulting from Equation (20). The resulting system of equations is non-linear. Its matrix of coefficients, with the dimensions of $(N_I+1) \times (N_I+1)$ is very sparse.

In the case of a channel network, the presented approach must be repeated for all branches. In this way, subsystems similar to Equations (22)–(23) are obtained for each channel. The subsystems describing subsequent branches must be assembled in order to obtain a global system for the entire network. In order to achieve this, we must apply Equations (15)–(16) for the channel junctions. Finally, we obtain the following global system of equations:

$$\boldsymbol{A}\boldsymbol{X} = \boldsymbol{B} \tag{24}$$

where $\boldsymbol{A}$ is the matrix consisting of matrices (22) obtained by applying the described approach to each channel in the network. Vectors $\boldsymbol{X}$ and $\boldsymbol{B}$ are constructed in a similar way. The vector of unknowns, $\boldsymbol{X}$, is obtained by concatenating the vectors of unknowns in each channel. Vector $\boldsymbol{B}$ contains the boundary condition values imposed on all channels in the network. The global system of non-linear equations with the introduced boundary conditions has the dimensions of $N_G \times N_G$ where:

$$N_G = \sum_{I=1}^{M}(N_I+1) \tag{25}$$

with M denoting the number of branches in the network. In other words the number of unknowns N_G is equal to the total number of cross-sections and channels in the network.

The resulting global system of non-linear equations must be solved using the iterative procedure. To this effect, we apply the Picard method with the modification proposed by Szymkiewicz [5]. In the modified Picard method the iterative procedure has the following form:

$$\boldsymbol{A}^* \boldsymbol{X}^{(m)} = \boldsymbol{B} \tag{26}$$

with

$$\boldsymbol{A}^* = \begin{cases} \boldsymbol{A}\left(\boldsymbol{X}^{(m)}\right) & \text{for } m=1 \\ \boldsymbol{A}\left(\frac{\boldsymbol{X}^{(m)}+\boldsymbol{X}^{(m-1)}}{2}\right) & \text{for } m>1 \end{cases} \tag{27}$$

where superscript m denotes the iteration index.

The stop condition is the simultaneous fulfillment of the following two criteria:

$$\left| h_i^{(m+1)} - h_i^{(m)} \right| \le \varepsilon_h \tag{28}$$

$$\left| Q_j^{(m+1)} - Q_j^{(m)} \right| \le \varepsilon_Q \tag{29}$$

$$(i=1,2,\ldots,N_j;\ j=1,2,\ldots,M),$$

where M denotes number of branches, N_j is the number of cross-sections of the jth branch, ε_h and ε_Q are water surface and discharge error tolerance respectively.

The computer code realizing the described algorithm has been implemented in Scilab language. The sparse system of linear equations arising at each iteration was solved using $\boldsymbol{LU}$ decomposition.

4. Discussion of obtained results of computations

We validated the proposed method of solution on an arbitrarily chosen channel network (*cf.* Figure 6), consisting of 24 rectangular channels with constant values of bed slopes and Manning's roughness coefficients. Spatial discretization was carried out with a constant value of $\Delta x = 10\,\mathrm{m}$, identical for each channel. Other characteristics of the channel network in question are given in Table 1.
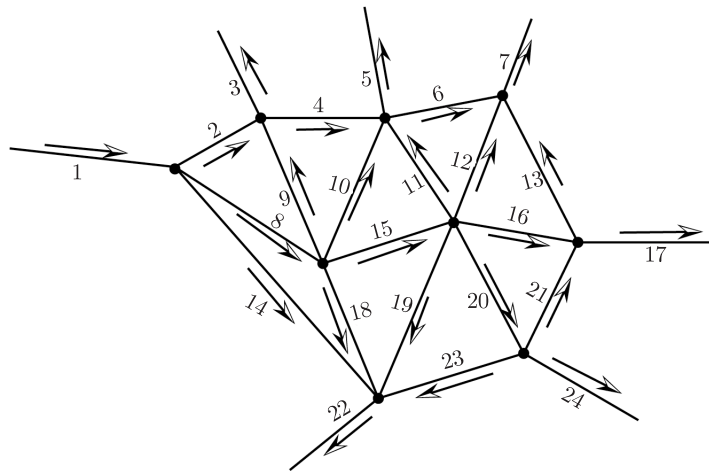

Figure 6. Assumed channel network (arrows denote the assumed positive flow direction)

The initial approximation of the water stage values in each cross-section was the sum of the bed level and of the depth imposed at its end. For the channels with no imposed boundary conditions, the initial estimation of water surface levels corresponded to a depth of $H^{(0)} = 1.5\,\mathrm{m}$. The initial estimation of the discharge values for each channel was obtained using the Manning formula, as in the case of the calculations of steady uniform flow. The boundary conditions corresponding to the water surface levels imposed at all pendant nodes are listed in Table 2. The computations were performed with a tolerance $\varepsilon_h = 0.001\,\mathrm{m}$ and $\varepsilon_Q = 0.01\,\mathrm{m^3/s}$.

The computed values of flow rate Q and water stages at the upstream (h_U) and downstream (h_D) end of each channel are presented in Table 3. The computations were terminated after 14 iterations.

For comparison, the problem under study was solved using the energy equation [5]. The same initial estimation of discharge and water stage values was used together with the same error tolerance criteria. The comparison of discharge values obtained using both approaches showed no significant differences. The maximum observed difference between the values of the calculated discharge was $\Delta Q_{\mathrm{max}} = 0.135\,\mathrm{m^3/s}$, corresponding to a relative error of about 2.5%. Similarly,

Table 1. Hydraulic characteristics of the channel network

No.	Bed slope s (–)	Bed width B (m)	Manning's coefficient n (s/m$^{1/3}$)	Channel length L (m)
1	0.0001	6.0	0.02	1000
2	0.0005	4.0	0.02	500
3	0.001	2.0	0.03	500
4	0.0005	3.5	0.02	500
5	0.001	2.0	0.03	500
6	0.0005	3.2	0.02	500
7	0.001	2.0	0.03	500
8	0.0001	3.0	0.02	1000
9	0.00015	2.0	0.025	1000
10	0.0004	2.0	0.025	1000
11	0.0003	2.0	0.025	1000
12	0.00055	2.0	0.025	1000
13	0.00045	3.0	0.025	1000
14	0.00025	2.8	0.02	2000
15	0.0001	2.5	0.02	1000
16	0.0001	3.0	0.02	1000
17	0.0001	2.0	0.02	1000
18	0.0004	2.0	0.03	1000
19	0.0003	2.0	0.025	1000
20	0.001	2.0	0.025	1000
21	−0.0018	2.0	0.02	500
22	0.001	2.0	0.03	750
23	−0.0014	2.0	0.02	500
24	0.001	2.0	0.02	750

Table 2. Boundary conditions imposed at the pendant nodes

Channel No.	Depth (m)
1	2.0
3	1.5
5	1.5
7	1.5
17	1.5
22	1.5
24	1.5

Table 3. Calculated flow-discharge values and water levels

Channel No.	Q ($\mathrm{m^3/s}$)	h_U (m)	h_D (m)
1	13.566	102.00	101.42
2	6.994	101.44	101.10
3	2.183	101.13	100.65
4	4.376	101.12	100.94
5	2.400	100.95	100.40
6	2.481	100.96	100.90
7	3.018	100.88	100.15
8	3.342	101.46	101.09
9	−0.434	101.11	101.14
10	0.983	101.11	100.96
11	−0.478	100.92	100.96
12	0.368	100.92	100.90
13	0.169	100.91	100.90
14	3.230	101.46	100.89
15	1.858	101.11	100.92
16	0.502	100.92	100.90
17	−1.681	100.90	101.00
18	0.935	101.11	100.90
19	0.304	100.92	100.91
20	1.162	100.92	100.75
21	−2.014	100.75	100.89
22	2.228	100.89	100.15
23	−2.242	100.74	100.89
24	5.417	100.70	99.45

the computed flow profiles did not differ significantly either, with the greatest difference between the computed water surface levels being $\Delta h_{\max} = 0.051\,\mathrm{m}$ (Figure 7).

Although the difference between the solution of the dynamic and energy equation was not significant in terms of numerical values, and although both approaches can be deemed equivalent, the reason for the observed difference is definitely worth investigating.

One can expect that the solution of the same problem should not be different, regardless of whether Equation (4) or Equation (11) is used. Particularly so, if one of these equations can be derived from the other. However, the differences may arise from the approximation used in the applied numerical method.
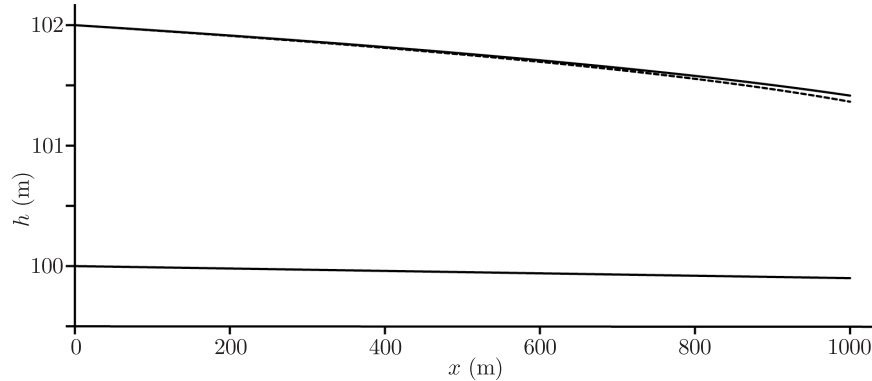
Figure 7. Computed flow profiles in channel 1: dotted line – Equation (4),
solid line – Equation (11)

Let us reconsider the discrete form of the dynamic equation (20):

$$(h_{i+1} - h_i) + \frac{2\beta \cdot Q^2}{g(A_i + A_{i+1})} \left(\frac{1}{A_{i+1}} - \frac{1}{A_i} \right) + \frac{\Delta x}{2} \left(\frac{|Q|Q \cdot n_i^2}{A_i^2 \cdot R_i^{4/3}} + \frac{|Q|Q \cdot n_{i+1}^2}{A_{i+1}^2 \cdot R_{i+1}^{4/3}} \right) = 0 \quad (30)$$

The difference approximation of the energy equation (4) is given as follows [1, 5]:

$$(h_{i+1} - h_i) + \frac{\alpha \cdot Q^2}{2g} \left(\frac{1}{A_{i+1}^2} - \frac{1}{A_i^2} \right) + \frac{\Delta x}{2} \left(\frac{|Q|Q \cdot n_i^2}{A_i^2 \cdot R_i^{4/3}} + \frac{|Q|Q \cdot n_{i+1}^2}{A_{i+1}^2 \cdot R_{i+1}^{4/3}} \right) = 0 \quad (31)$$

Certain terms of both difference equations are similar, but their middle terms are
different. After subtracting one equation from the other, the following relation is
obtained:

$$\Delta = \frac{\alpha}{2} \left(\frac{1}{A_{i+1}^2} - \frac{1}{A_i^2} \right) - \frac{2\beta}{(A_i + A_{i+1})} \left(\frac{1}{A_{i+1}} - \frac{1}{A_i} \right) \quad (32)$$

If Equation (30) and Equation (31) are equivalent the obtained difference Δ
should vanish. However from Equation (32) it follows that $\Delta \neq 0$. This means
that although the ordinary differential equations (4) and (11) are equivalent (one
can be derived from the other), their difference approximations are not. The
above relation (32) shows that the discrete forms of dynamic and energy equations
differ. Consequently, slightly different results can be obtained from these difference
equations. This corresponds to the conclusions presented by Cunge *et al.* in [6].
When discussing the problem of the analysis of SGV flow, they suggested using
the Saint-Venant equations with imposed, time-independent boundary conditions.
However, they discovered that this approach is inconsistent with the discrete form
of the energy equation (4) when applied to SGV flow.

5. Conclusions

The analysis of steady gradually varied flow can be carried out using either
the energy equation (4) or the dynamic equation (11). Although these equations
are equivalent, and although in both cases the same modified Picard method

was used to solve the system of non-linear equations that arises, their numerical solutions differ. This insignificant difference results from the inconsistency of the discrete forms of the dynamic and energy equations, obtained with the finite difference method.

Acknowledgements

References

[1] Szymkiewicz R 2010 *Numerical Modeling in Open Channel Hydraulics*, Springer
[2] Chow V T 1959 *Open-channel Hydraulics*, McGraw-Hill Book Company
[3] Chanson H 2004 *The Hydraulics of Open-channel Flow: an Introduction*, Second Edition, Elsevier
[4] Ascher U M and Petzold L R 1998 *Computer Methods for Ordinary Differential Equations and Differential-algebraic Equations*, SIAM
[5] Szymkiewicz A and Szymkiewicz R 2004 *Commun. Num. Meth. Engng* **20** (4) 299
[6] Cunge J A, Holly F M and Verwey A 1979 *Practical Aspects of Computational River Hydraulics*, Pitman Advanced Publishing Program